JOC Article
pubs.acs.org/joc

Site-Selective Bimodal Absorption and Emission of Distonic Radical Cation

Sachiko Tojo, Mamoru Fujitsuka, and Tetsuro Majima*

The Institute of Scientific and Industrial Research (SANKEN), Osaka University Mihogaoka 8-1, Ibaraki, Osaka 567-0047, Japan

majima@sanken.osaka-u.ac.jp

Received March 5, 2010

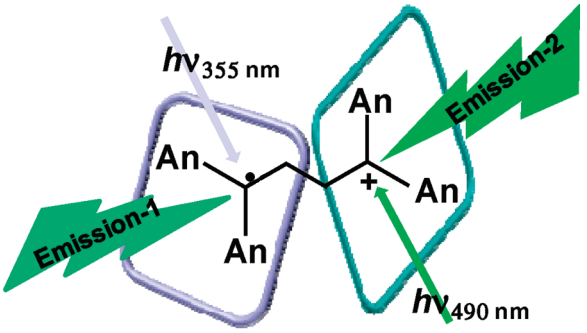

Spin and positive charge localized

The bimodal emissions by the site-selective excitation

An acyclic 1,4-distonic dimer radical cation ($DAE_2^{\bullet+}$) was generated from the dimerization of 1,1-bis(4-methoxyphenyl)ethylene radical cation ($DAE^{\bullet+}$) with the neutral molecule (DAE) in solution. The absorption spectrum of $DAE_2^{\bullet+}$ shows bimodal absorption bands with peaks at 350 and 500 nm corresponding to the 1,1-bis(4-methoxyphenyl)ethyl radical ($An_2C^{\bullet}CH_3$) and 1,1-bis(4-methoxyphenyl)ethyl cation ($An_2C^{+}CH_3$), respectively. Therefore, $DAE_2^{\bullet+}$ in the ground state has the spin and positive charge localized on the 1- and 4-positions, respectively. The bimodal characteristic emissions by the site-selective excitation of radical and cation sites of $DAE_2^{\bullet+}$ were observed at 77 K, showing that the excitation energy is localized on the radical or cation site of $DAE_2^{\bullet+}$ in the excited state. The interaction between radical and cation sites of $DAE_2^{\bullet+}$ in the ground and excited states are discussed on the basis of the steady-state spectroscopic and transient absorption measurements, as well as theoretical calculations.

Introduction

Radical cations have bimodal reactivities as radical and cation, showing various unimolecular and bimolecular reactions such as isomerization, dimerization, deprotonation, decomposition, rearrangement, and addition to nucleophiles.[1] The distributions of spin and charge are generally overlapped in the radical cations, and the reactivities depend on the structure and substituent. On the other hand, distonic radical cations having radical and positive charge sites separately are suggested.[2−4] Distonic radical cations have been suggested and evidenced for many radical cations in the gas phase by studies using mass spectroscopy and so on.[5−8] In solution, although no direct evidence has been shown for distonic radical cations, various distonic radical cations have

(1) Schmittel, M.; Burghart, A. *Angew. Chem., Int. Ed. Engl.* **1997**, *36*, 2551.
(2) Mizuno, K.; Tamai, T.; Hashida, I.; Otsuji, Y.; Kuriyama, Y.; Tokumaru, K. *J. Org. Chem.* **1994**, *59*, 7329.
(3) Tamai, T.; Ichinose, N.; Tanaka, T.; Sasuga, T.; Hashida, I.; Mizuno, K. *J. Org. Chem.* **1998**, *63*, 3204.
(4) Mizuno, K.; Tamai, T.; Hashida, I.; Otsuji, Y. *J. Org. Chem.* **1995**, *60*, 2935.
(5) Stirk, K. M.; Kiminkinen, L. K. M.; Kenttamaa, H. I. *Chem. Rev.* **1992**, *92*, 1649.
(6) Gozzo, F. C.; Moraes, L. A. B.; Eberlin, M. N.; Laali, K. K. *J. Am. Chem. Soc.* **2000**, *122*, 7776.
(7) Hammerum, S. *Mass Spectrom. Rev.* **1988**, *7*, 123.
(8) Gronert, S. *Chem. Rev.* **2001**, *101*, 329.

Published on Web 05/07/2010 DOI: 10.1021/jo1003949

been speculated to exist as intermediates in solution on the basis of product analysis.[9−11] For example, Newcomb et al. reported the reversible cyclization of alkene radical cation via a cyclic distonic radical cation in solution.[12] Fewer examples for the absorption and emission properties of the distonic radical cation have been reported.

The formation of aromatic distonic radical cation in solutions is unfavorable without a substituent stabilization of radical and/or cation sites. For example, introduction of a *p*-methoxyl group to an aromatic ring causes the stabilization of the cation and radical sites of the distonic radical cation. Therefore, it is expected that the distonic radical cation will be formed efficiently when a substrate has anisylmethyl sites even in solution.[13,14] Recently, Metzger et al. reported the formation of an acyclic distonic dimer radical cation of *trans*-anethole in solution based on the EESI-MS/MS measurement.[15,16] Takamuku et al. reported that the regioselective addition of O_2 toward *trans*-4-methoxylstilbene radical cation ($MOST^{\bullet+}$) occurs rapidly, because of the charge-spin separation and localization of an unpaired electron on the β-olefinic carbon, whereas *trans*-stilbene radical cation ($ST^{\bullet+}$) has little reactivity toward O_2.[17] Elucidation of the properties of distonic radical cations is necessary for understanding the site selective reactivity of radical cation.

Fewer physical and chemical properties of excited radical ions, such as fluorescence, have been revealed. Usually excited radical ions have weak or nonfluorescent nature and extremely short lifetimes, typically much shorter than 1 ns.[18−20] Only a few radical cations have been reported to show fluorescence in solution.[21,22] Usually, assignment of fluorescence from radical cations in the excited state is difficult because of the formation of fluorescent byproduct, as has been already pointed out by Fox.[23]

Contrary to radical cations, the spectroscopic properties of free-radical or carbon-centered cations in ground and excited states have been extensively studied under various conditions.[24−28] Turro et al. reported the independent formation of diphenylmethyl radical and cation in zeolites based on spectroscopic measurement.[29] No interaction was observed between the free radical and cation in both the ground and excited states inside the zeolites.

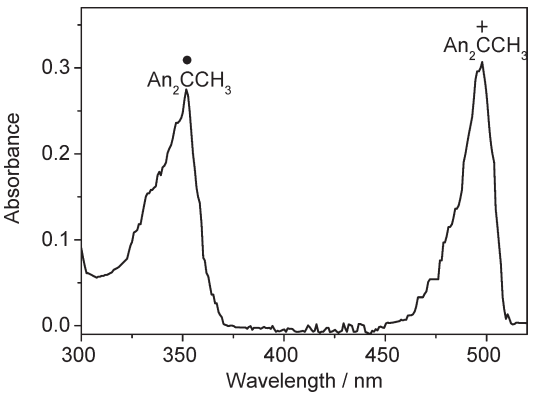

FIGURE 1. Steady-state absorption spectrum of $An_2C^{\bullet}CH_3$ and $An_2C^{+}CH_3$ observed after γ-irradiation of An_2CHCH_3 (10 mM) in *n*-BuCl rigid glass at 77 K.

In particular, a little has been known on the absorption and emission properties of the distonic radical cation, while both cooperative and independent interactions have been suggested on the basis of product analysis. Thus, it is important to elucidate the interaction of these sites and to differentiate from the corresponding free radical and cation. This issue will be clarified by emission spectroscopy. If the radical and cation sites have no interaction even in the excited state, bimodal emissions from the radical and cation sites in distonic radical cation will be observed upon the site-selective excitation.

In this work, we report the bimodal absorptions and the emissions from the site-selective excitation of the radical and cation site of an acyclic 1,4-dimer radical cation, $DAE_2^{\bullet+}$, which was indicated as an intermediate to produce the 1,2-dioxane via addition of molecular oxygen during the photooxygenation of aromatic alkene radical cation.[30] This is the first example of bimodal emissions of distonic radical cation.

Results and discussion

Absorption and Emission of Free Radical and Cation at 77 K. To observe the absorption and emission of 1,1-bis(4-methoxyphenyl)ethyl radical ($An_2C^{\bullet}CH_3$) and 1,1-bis(4-methoxyphenyl)ethyl cation ($An_2C^{+}CH_3$), we examined γ-irradiation of *n*-butyl chloride (*n*-BuCl) rigid glass containing An_2CHCH_3 (1×10^{-2} M) at 77 K. Figure 1 shows the absorption spectrum with two peaks (λ_{max}) at 350 and 500 nm assigned to the D_2-D_0 absorption of $An_2C^{\bullet}CH_3$ and the S_1-S_0 absorption of $An_2C^{+}CH_3$, respectively.[31]

Figure 2a shows the D_1-D_0 fluorescence spectrum with a peak at 533 nm and characteristic vibrational bands at the

(9) Bouchoux, G.; Berruyer, F.; Hiberty, P. C.; Wu, W. *Chem.—Eur. J.* **2007**, *13*, 2912.
(10) Janovsky, I.; Knolle, W.; Naumov, S.; Williams, F. *Chem.—Eur. J.* **2004**, *10*, 5524.
(11) O'Neil, L. L.; Wiest, O. *J. Org. Chem.* **2006**, *71*, 8926.
(12) Horner, J. H.; Newcomb, M. *J. Org. Chem.* **2007**, *72*, 1609.
(13) Tojo, S.; Morishima, K.; Ishida, A.; Majima, T.; Takamuku, S. *J. Org. Chem.* **1995**, *60*, 4684.
(14) Majima, T.; Tojo, S.; Ishida, A.; Takamuku, S. *J. Org. Chem.* **1996**, *61*, 7793.
(15) Marquez, C. A.; Wang, H.; Fabbretti, F.; Metzger, J. O. *J. Am. Chem. Soc.* **2008**, *130*, 17208.
(16) Meyer, S.; Koch, R.; Metzger, J. O. *Angew. Chem., Int. Ed.* **2003**, *42*, 4700.
(17) Majima, T.; Tojo, S.; Ishida, A.; Takamuku, S. *J. Phys. Chem.* **1996**, *100*, 13615.
(18) Zimmer, K.; Godicke, B.; Hoppmeier, M.; Meyer, H.; Schweig, A. *Chem. Phys.* **1999**, *248*, 263.
(19) Ishida, A.; Fukui, M.; Ogawa, H.; Tojo, S.; Majima, T.; Takamuku, S. *J. Phys. Chem.* **1995**, *99*, 10808.
(20) Cai, X.; Sakamoto, M.; Fujitsuka, M.; Majima, T. *J. Phys. Chem. A* **2007**, *111*, 1788.
(21) Ichinose, N.; Tanaka, T.; Kawanishi, S.; Suzuki, T.; Endo, K. *J. Phys. Chem. A* **1999**, *103*, 7923.
(22) Ichinose, N.; Tojo, S.; Majima, T. *Chem. Lett.* **2000**, 1126.
(23) Breslin, D. T.; Fox, M. A. *J. Phys. Chem.* **1994**, *98*, 408.
(24) Das, P. K. *Chem. Rev.* **1993**, *93*, 119.
(25) Boyd, M. K. *Mol. Supramol. Photochem.* **1997**, *1*, 147.
(26) Weir, D.; Johnston, L. J.; Scaiano, J. C. *J. Phys. Chem.* **1988**, *92*, 1742.
(27) Sakamoto, M.; Cai, X.; Fujitsuka, M.; Majima, T. *J. Phys. Chem. A* **2006**, *110*, 9788.
(28) Hara, M.; Tojo, S.; Majima, T. *J. Phys. Chem. A* **2003**, *107*, 4778.
(29) Jockusch, S.; Hirano, T.; Liu, Z.; Turro, N. J. *J. Phys. Chem. B* **2000**, *104*, 1212.
(30) Fujita, M.; Shindo, A.; Ishida, A.; Majima, T.; Takamuku, S.; Fukuzumi, S. *Bull. Chem. Soc. Jpn.* **1996**, *69*, 743.
(31) Popielarz, R.; Arnold, D. R. *J. Am. Chem. Soc.* **1990**, *112*, 3068.

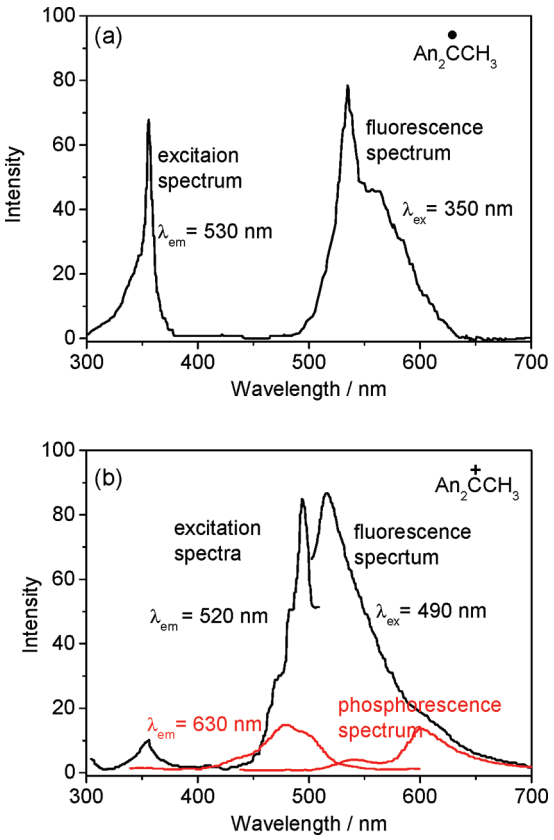

FIGURE 2. Steady-state fluorescence excitation (λ_{em} = 530 nm) and emission (λ_{ex} = 350 nm) spectra of $An_2C^{\bullet}CH_3$ (a) and fluorescence and phosphorescence excitation (λ_{em} = 490 nm) and emission (λ_{ex} = 520 and 630 nm) spectra of $An_2C^{+}CH_3$ (b) at 77 K.

longer wavelength around 550−600 nm (τ = 285 ns, ϕ = 0.18) by the excitation of $An_2C^{\bullet}CH_3$ at 350 nm. Figure 2b shows the S_1-S_0 fluorescence spectrum with a peak at 515 nm (τ < 4 ns, ϕ = 0.27) and the T_1-S_0 phosphorescence spectrum with a peak at 600 nm (τ = 2.5 ms) by the excitation of $An_2C^{+}CH_3$ at 490 nm. It was indicated that $An_2C^{+}CH_3$ in the singlet excited state transforms partly to that in the triplet excited state which emits the T_1-S_0 phosphorescence. The excitation spectrum of each emission was in good agreement with the absorption spectrum of the corresponding species.

Formation and Reactivity of 1,4-Distonic Radical Cation. The transient absorption spectra recorded at various times after an 8-ns electron pulse during the pulse radiolysis of DAE in benzonitrile (BN) at room temperature under Ar atmosphere are shown in Figure 3. The transient absorption bands of $DAE^{\bullet+}$ around 390, 590, and 1600 nm were observed at 50 ns after the pulse. The observed spectrum was the same as that reported for DAE in 1,2-dichloroethane at room temperature.[30] These bands of $DAE^{\bullet+}$ decayed with simultaneous formation of the two bands at 350 and 500 nm in the same time scale (Figure 3a). The formation rate of 500 nm increased with increasing the concentration of DAE, indicating that $DAE^{\bullet+}$ reacts with a neutral DAE to give DAE dimer radical cation ($DAE_2^{\bullet+}$) at the dimerization rate constant of 1.2×10^9 M^{-1} s^{-1} in BN (eq 4). No CR band was observed for $DAE_2^{\bullet+}$ in the near-infrared region (Figure 3b), suggesting that $DAE_2^{\bullet+}$ is not a π-dimer radical cation like the naphthalene dimer radical cation ($Np_2^{\bullet+}$)[32] but a σ-dimer radical cation having σ-bonding character as discussed below.

The two bands at 350 and 500 nm of $DAE_2^{\bullet+}$ showed different decay kinetics as shown in Figure 4. The absorption band at 350 nm showed two decay processes. The fast and slow decay constants were calculated to be 8.9×10^5 and $< 2.0 \times 10^4$ s^{-1}, respectively. On the other hand, a second-order fit can be applied to the decay of absorption band at 500 nm, indicating that the absorption band at 500 nm decays bimolecularly by the neutralization with $BN^{\bullet-}$ (eq 6). Therefore, it is suggested that $DAE_2^{\bullet+}$ has two different chromophores that are spatially separated in $DAE_2^{\bullet+}$. In order to elucidate the site-selective reactivities of $DAE_2^{\bullet+}$, the pulse radiolysis of DAE was performed in the presence of O_2 or methanol (MeOH).

In the presence of O_2 under the same experimental conditions, the absorption band at 350 nm of $DAE_2^{\bullet+}$ decays rapidly, accompanied by the concomitant appearance of a new absorption band at 520 nm (Figure 5).[33] The rate constant for the reaction of $DAE_2^{\bullet+}$ with O_2 in BN was determined from the decay at 350 nm and the formation at 520 nm to be $k_{O_2} > 10^9$ M^{-1} s^{-1}. The similar rate constant ($k_{O_2} > 10^9$ M^{-1} s^{-1}) for the reaction of $An_2CH^{\bullet}$ with O_2 in BN was observed.[34] The spectral change of $DAE_2^{\bullet+}$ in the presence of O_2 clearly indicates the formation of the addition product between O_2 and $DAE_2^{\bullet+}$ with the localized unpaired electron. The similar phenomenon was observed for the reaction of trimesitylphosphine radical cation with O_2, where the radical cation having a peak at 600 nm reacts with O_2 to give the peroxyl radical cation with a peak at 570 nm, assigned to the P-centered cation.[35] In addition, the second-order rate constant of $DAE_2^{\bullet+}$ with O_2 was similar to that of trianisylphosphine radical cation with O_2 ($k_{O_2} = 1.9 \times 10^9$ M^{-1} s^{-1}). The absorption spectrum with a peak at 520 nm observed by the addition of O_2 can be reasonably assigned to the cation site of a peroxyl radical cation of the oxygen adduct, since the peroxyl radical $An_2CHOO^{\bullet}$ generated from the reaction of free $An_2CH^{\bullet}$ with O_2 has no absorption in the visible regions (eq 5).

In the presence of MeOH as a nucleophile under the same experimental condition, the transient optical densities (ΔOD) of $DAE_2^{\bullet+}$ decreased because $BN^{\bullet+}$ is partly trapped by MeOH. No effect of MeOH was observed on the decay profile at 350 nm. The decay rate of $DAE_2^{\bullet+}$ at 500 nm was not accelerated by addition of MeOH. The bimolecular rate constant was estimated to be $k_{MeOH} < 10^5$ M^{-1} s^{-1}. The rate constant for the reaction of An_2CH^{+} with MeOH in BN was determined to be $k_{MeOH} = 2.9 \times 10^5$ M^{-1} s^{-1}. In addition, the decay rate of $DAE_2^{\bullet+}$ at 500 nm did not increase with increasing the concentration of DAE as a nucleophile. The present observations indicated that the

(32) Cai, X.; Tojo, S.; Fujitsuka, M.; Majima, T. *J. Phys. Chem. A* **2006**, *110*, 9319.

(33) Pulse radiolysis of 1,1,2,2-tetraanisylethane (TAE) was carried out in BN at room temperature. $TAE^{\bullet+}$ undergoes C−C bond cleavage to yield $An_2CH^{\bullet}$ and An_2CH^{+}. In the presence of O_2, $An_2CH^{\bullet}$ was scavenged by O_2, but the shift of absorption band for free $An_2C^{+}H$ was not observed.

(34) The rate constants with O_2 could not determine because the transient absorption bands at 350 nm of $DAE_2^{\bullet+}$ and $An_2CH^{\bullet}$ rapidly decayed (< 50 ns) under even the air atmosphere.

(35) Tojo, S.; Yasui, S.; Fujitsuka, M.; Majima, T. *J. Org. Chem.* **2006**, *71*, 8227.

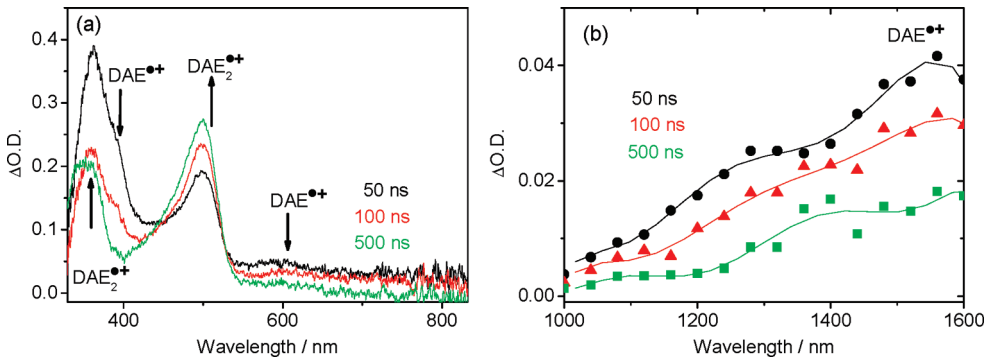

FIGURE 3. Transient absorption spectra obtained at 50 (black circle), 100 (red triangle), and 500 ns (green square) after an electron pulse of DAE 7.5 mM in BN in the visible region (a) and in the near-infrared region (b).

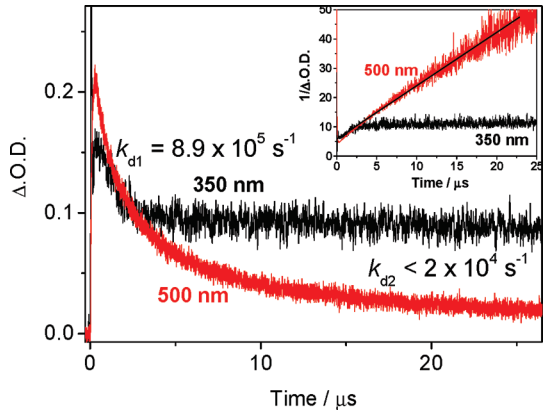

FIGURE 4. Time profiles of the transient absorption at 350 (black) and 500 nm (red) after an electron pulse of DAE 7.5 mM in BN. The inset shows the second-order plots for the decay kinetics of $DAE_2^{\bullet+}$ at 350 (black) and 500 nm (red).

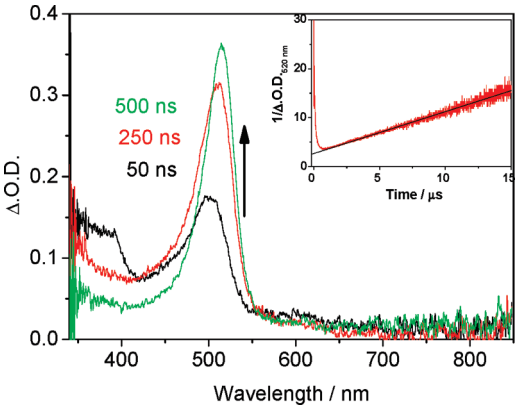

FIGURE 5. Transient absorption spectra obtained at 50 (black), 250 (red), and 500 ns (green) after electron pulse of DAE 7.5 mM in BN in the presence of O_2. The inset shows the second-order plots for the decay kinetics at 520 nm (red).

transient of 500 nm has a rather low reactivity compared with that of 350 nm.

$$BN \rightsquigarrow BN^{\bullet+} + e^- \quad (1)$$

$$e^- + BN \rightarrow BN^{\bullet-} \quad (2)$$

$$BN^{\bullet+} + DAE \rightarrow DAE^{\bullet+}(An_2C{=}CH_2^{\bullet+}) \quad (3)$$

$$DAE + DAE^{\bullet+} \rightarrow DAE_2^{\bullet+}(An_2C^{\bullet}CH_2CH_2C^{+}An_2) \quad (4)$$

$$DAE_2^{\bullet+} + O_2 \rightarrow 1,6\text{-peroxyl radical cation } (An_2C(OO^{\bullet})CH_2CH_2C^{+}An_2) \quad (5)$$

$$DAE_2^{\bullet+} + BN^{\bullet-} \rightarrow \text{neutralization product(s)} \quad (6)$$

$DAE^{\bullet+}$ was generated by γ-radiolysis (4.5×10^6 Gy) in *n*-BuCl rigid glass at 77 K (Figure 6, black line). The absorption spectral change was observed upon warming from 77 to 100 K. The absorption band of $DAE^{\bullet+}$ disappeared upon warming of the rigid glass, together with the formation of sharp absorption bands at λ_{max} 350 and 500 nm (Figure 6, red line).

$$n\text{-BuCl} \rightsquigarrow n\text{-BuCl}^{\bullet+} + e^- \quad (7)$$

$$n\text{-BuCl}^{\bullet+} + DAE \rightarrow DAE^{\bullet+} \quad (8)$$

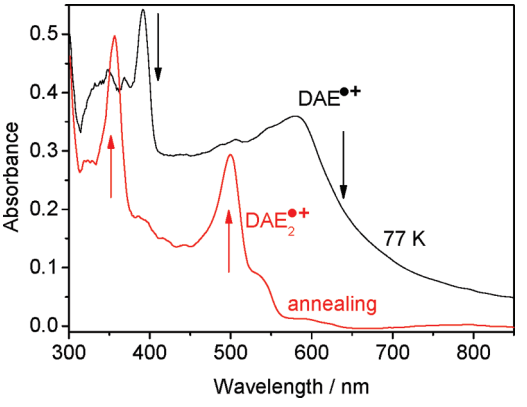

FIGURE 6. Steady-state absorption spectra of $DAE^{\bullet+}$ and $DAE_2^{\bullet+}$ observed after γ-irradiation of DAE (10 mM) in *n*-BuCl rigid glass under vacuum at 77 K.

The absorption band at λ_{max} 350 nm is similar to that of $An_2C^{\bullet}CH_3$. On the other hand, the absorption band at λ_{max} 500 nm is similar to that of $An_2C^{+}CH_3$. The absorption spectrum of $DAE_2^{\bullet+}$ can be explained on the basis of the superposition of the absorption of dianisylethyl radical ($An_2C^{\bullet}CH_3$, 350 nm) and dianisylethyl cation ($An_2C^{+}CH_3$, 500 nm) chromophores, indicating that the radical and cation sites are distributed to subunits I and II, respectively (Scheme 1). These results suggest that $DAE_2^{\bullet+}$ generated

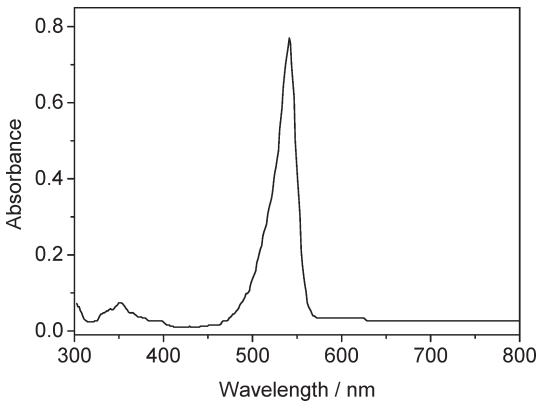

FIGURE 7. Steady-state absorption spectrum of 1,6-peroxyl radical cation of $DAE_2^{\bullet+}$ ($An_2C(OO^{\bullet})CH_2CH_2C^{+}An_2$) observed after γ-irradiation of DAE (10 mM) in *n*-BuCl rigid glass in the presence of O_2 at 77 K.

SCHEME 1. Generation of Distonic Radical Cations from the Dimerization of $DAE^{\bullet+}$

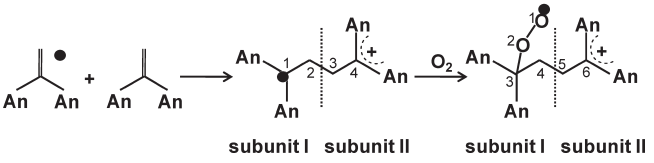

through C−C bond formation between β-carbons of DAE is a 1,4-distonic radical cation with an acyclic linear structure (Scheme 1).

In the presence of O_2, the radical site with λ_{max} at 350 nm disappeared upon warming of the rigid glass. The radical site of $DAE_2^{\bullet+}$ was scavenged by O_2 completely to form the new absorption band with a peak at 520 nm and weak absorption around 350 nm (Figure 7), which is consistent with the results of the pulse radiolysis at room temperature. This result suggests that the absorption band at λ_{max} 520 nm is assigned to the cation site of 1,6-distonic peroxyl radical cation with an acyclic structure formed by the addition of O_2 to subunit I of radical site of $DAE_2^{\bullet+}$ (Scheme 1).

Reactivity of 1,6-Peroxyl Distonic Radical Cation. As shown in the inset of Figure 5, the second-order decay of a 1,6-peroxyl distonic radical cation was similar to that of the cation site of $DAE_2^{\bullet+}$. In order to elucidate the reactivity of 1,6-peroxyl distonic radical cation, pulse radiolysis of DAE was performed in the presence of MeOH. In the presence of MeOH, decay of the cation site of the 1,6-peroxyl distonic radical cation monitored at 520 nm was not accelerated by addition of MeOH ($k_{MeOH} < 10^5$ M^{-1} s^{-1}). This phenomenon was similar to that of the cation site of $DAE_2^{\bullet+}$.

Emission of 1,4-Distonic Radical Cation at 77 K. Generally radical cations have no emission. Similarly, no emission was observed with $DAE^{\bullet+}$ generated by the γ-irradiation in *n*-BuCl rigid glass at 77 K. On the other hand, the emissions dependent on the excitation wavelength were observed with $DAE_2^{\bullet+}$ at 77 K. The fluorescence spectrum displayed a peak (λ_f) at 533 nm and characteristic vibrational bands around 550−600 nm (τ_f = 189 ns, ϕ = 0.12) by the selective excitation of the radical site of $DAE_2^{\bullet+}$ (λ_{max} = 350 nm) (Figure 8). The fluorescence properties were similar to those of $An_2C^{\bullet}CH_3$ (λ_f = 500 and 520−600 nm, τ_f = 285 ns,

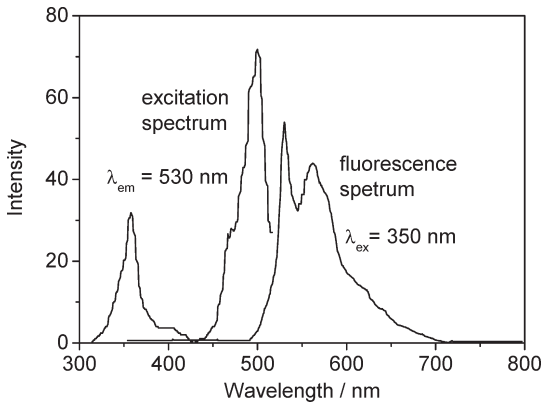

FIGURE 8. Steady-state fluorescence excitation (λ_{em} = 530 nm) and emission (λ_{ex} = 350 nm) spectra of radical site of $DAE_2^{\bullet+}$ ($An_2C^{\bullet}H$) at 77 K.

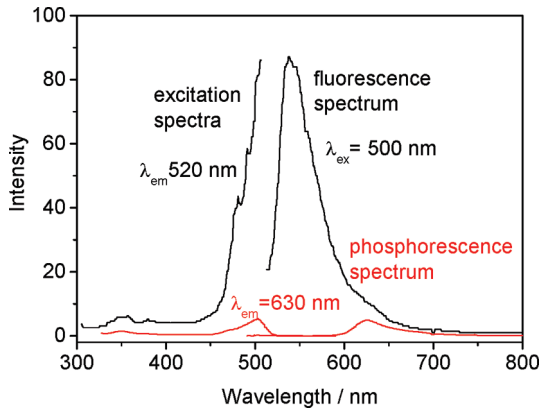

FIGURE 9. Steady-state fluorescence (black) and phosphorescence (red) excitation (λ_{em} = 500 nm) and emission (λ_{ex} = 520 and 630 nm) spectra of cation site of $DAE_2^{\bullet+}$ ($An_2C^{+}H$) at 77 K.

ϕ = 0.18), showing that the selective excitation of the radical site of $DAE_2^{\bullet+}$ results in the emission from the radical site. Therefore, the excitation energy is localized on the radical site of $DAE_2^{\bullet+}$, and no excitation energy transfer occurs from the radical site to the cation site in $DAE_2^{\bullet+}$.

The fluorescence with a λ_f at 520 nm (τ_f < 4 ns, ϕ = 0.12) and the phosphorescence with a peak (λ_p) at 630 nm (τ_p = 2.5 ms) were observed by the selective excitation of the cation site at 490 nm, tuned to the absorption of the cation site of $DAE_2^{\bullet+}$ (Figure 9). The properties of fluorescence and phosphorescence generated by the selective excitation of the cation site of $DAE_2^{\bullet+}$ were similar to those of $An_2C^{+}CH_3$ (λ_f = 515 nm, τ_f < 4 ns, ϕ = 0.27, λ_p = 600 nm, and τ_p = 2.5 ms). The excitation spectrum with peaks at 350 and 500 nm was observed for the fluorescence at 520 nm and the phosphorescence at 600 nm. Ikeda et al. reported that diphenylethyl cation possessed absorption bands with two peaks at 314 and 424 nm.[36] The results also suggest that the observed weak excitation band at 350 nm is assigned to the cation site rather than the radical site of $DAE_2^{\bullet+}$, which is also supported by the fact that the phosphorescence was not observed by the selective excitation of the radical site of $DAE_2^{\bullet+}$. It was indicated that no interaction exists between the radical and cation sites of $DAE_2^{\bullet+}$ in the excited state.

(36) Ikeda, H.; Tanaka, F.; Kabuto, C. *Tetrahedron Lett.* **2005**, *46*, 2663.

CHART 1

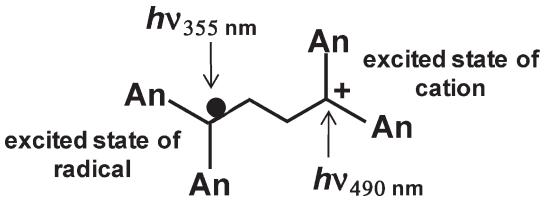

It is concluded that the radical and cation sites in $DAE_2^{\bullet+}$ can be selectively excited by the excitation at 350 and 490 nm, respectively (Chart 1). The excitation at 350 nm generates the D_1-D_0 fluorescence after the internal conversion from the initially generated the D_2 state of radical site of $DAE_2^{\bullet+}$. The excitation at 490 nm generates the S_1-S_0 fluorescence and T_1-S_0 phosphorescence from the cation site of $DAE_2^{\bullet+}$, indicating the contribution of the intersystem crossing from S_1 to T_1 of cation site.

Emission of 1,6-Distonic Peroxyl Radical Cation at 77 K. In the presence of O_2, the S_1-S_0 fluorescence with a peak at 560 nm for the cation site was clearly observed without interference of emission from the radical site of a 1,6-distonic peroxyl radical cation (Figure 10) upon the selective excitation at 520 nm, tuned to the absorption of the cation site of a 1,6-distonic peroxyl radical cation. The fluorescence peak shifted to wavelength longer than that of $An_2C^+CH_3$. The excitation spectrum is in good agreement with the absorption spectrum observed. The T_1-S_0 phosphorescence was not observed because of the quenching of the triplet excited state by O_2.

Properties of Distonic Radical Cations in the Ground and Excited States. The present experimental results proved that two chromophores of $An_2C^{\bullet}$ and An_2C^+ linked by an ethylenyl group were independent in $DAE_2^{\bullet+}$ as a 1,4-distonic radical cation. The absorption and emission positions of the radical ($An_2C^{\bullet}$) and cation (An_2C^+) chromophores are summarized in Table 1.

The absorption bands with λ_{max} at 350 and 500 nm of $DAE_2^{\bullet+}$ are similar to those of the free radical and cation, respectively. Takamuku et al. observed an unusually long wavelength absorption band at 505 nm when 4-methoxystyrene and 1,2-bis(4-methoxyphenyl)cyclobutane were independently subjected to pulse radiolysis in 1,2-dichloroethane.[37] They assigned the band to the 1,4-diarylbutane-1,4-diyl radical cation in which radical site ($AnC^{\bullet}H$) and cation site (AnC^+H) do not exist separately. However, the absorption spectra of $DAE_2^{\bullet+}$ have dual characteristics that correspond to both the radical and the cation subunits. The bimodal reactivities of $DAE_2^{\bullet+}$ toward O_2 and MeOH were similar to those of the free $An_2CH^{\bullet}$ and An_2CH^+. The reactivity toward O_2 for $DAE_2^{\bullet+}$ is higher than that for the general aromatic radical cation. This result suggests that an unpaired electron is localized on the sp^3 carbon in the radical site (subunit I in Scheme 1). On the other hand, the low electrophilic reactivity of the cation site of $DAE_2^{\bullet+}$ is similar to that of an aromatic radical cation

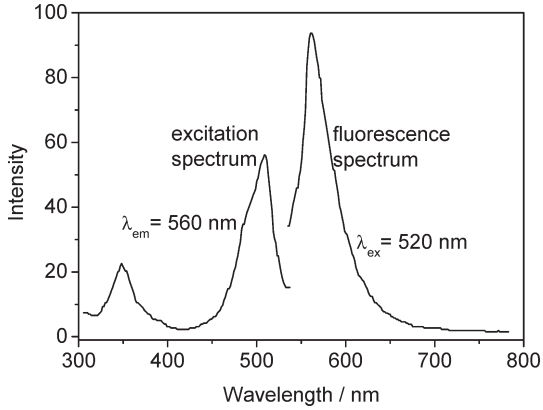

FIGURE 10. Steady-state fluorescence excitation (λ_{em} = 520 nm) and emission (λ_{ex} = 560 nm) spectra of cation site of 1,6- peroxyl radical cation of $DAE_2^{\bullet+}$ at 77 K.

derivative substituted with a *p*-methoxy group such as $An_2CHCH_3^{\bullet+}$ with MeOH.[38] Similarly, the reactivity of $MOST^{\bullet+}$ with MeOH was lower than that of $ST^{\bullet+}$ in BN.[39] This result suggests that the positive charge in the cation site of $DAE_2^{\bullet+}$ is delocalized on two 4-methoxyphenyl groups (subunit II in Scheme 1). These results suggest that no interaction exists between the radical and cation sites of extended acyclic $DAE_2^{\bullet+}$ in the ground state. $DAE_2^{\bullet+}$ exhibits the site-selective and bimodal reactivities at the radical and cation sites, independently. $DAE_2^{\bullet+}$ reacts selectively as either radical or carbocation, depending on the choice of the neutral reaction partner. The spin is localized on the C_1 of subunit I, and positive charge is delocalized in subunit II in the ground state, respectively.

The ϕ_f values for the excited radical and cation sites of $DAE_2^{\bullet+}$ were slightly smaller than those of $An_2CH^{\bullet}CH_3$ and $An_2CH^+CH_3$, respectively. However, the fluorescence and phosphorescence spectra obtained by the site-selective excitation of $DAE_2^{\bullet+}$ were almost equivalent with those of the free radical and cation. These results suggest that no interaction exists between the radical and cation sites of $DAE_2^{\bullet+}$ in the excited states, too.

The optimized structure and spin distribution of 1,6-distonic peroxyl radical cation calculated using the density functional theory is shown in Figure 11. The $C_1-C_2-C_3-C_4$ dihedral angle of 173.4° indicates the extended acyclic structure.

The calculated spin (ρ) and positive charge (q) densities of the 1,6-peroxyl radical cation of $DAE_2^{\bullet+}$ are shown in Figure 12. The spin densities at the two oxygen atoms of peroxyl group are +0.654 and +0.315, respectively, suggesting that the unpaired electron is mainly localized on the peroxyl moiety. In addition, the sum of the positive charge densities for subunit II is +0.768, indicating that positive charge is mainly delocalized on C_4 and two 4-methoxyphenyl groups on subunit II.

In the case of the cation sites of the 1,6-distonic peroxyl radical cation, the absorption and fluorescence peaks shifted to a wavelength longer than those of $An_2C^+CH_3$. This shift was not observed for $An_2C^+CH_3$ in the presence of O_2. The absorption and fluorescence peaks of the cation site

(37) Tojo, S.; Toki, S.; Takamuku, S. *J. Org. Chem.* **1991**, *56*, 6240.

(38) Pulse radiolyses of An_2CHCH_3 was carried out in Ar-saturated BN at room temperature. The transient absorption band of $An_2CHCH_3^{\bullet+}$ around 450 nm was observed. The heterolytic and homolytic cleavage of the C-H bond of $An_2CHCH_3^{\bullet+}$ to form $An_2C^{\bullet}CH_3$ and $An_2C^+CH_3$ did not occur. The decay of $An_2CHCH_3^{\bullet+}$ at 450 nm was not accelerated by addition of MeOH (750 mM) ($k_{MeOH} < 10^5$ M^{-1} s^{-1}).

(39) Pulse radiolyses of MOST and ST were carried out in Ar-saturated BN at room temperature. Recations of $MOST^{\bullet+}$ and $ST^{\bullet+}$ with MeOH occur with rate constant of $k_r = 9.5 \times 10^5$, and 1.7×10^6 M^{-1} s^{-1}, respectively.

TABLE 1. Absorption and Emission Peaks (λ_{abs} and λ_{em}, Respectively) of Free Radical, Free Cation, and Distonic Radical Cation

	radical chromophore ($An_2C^{\bullet}$)		cation chromophore (An_2C^{+})	
	λ_{abs}/nm	λ_{em}/nm	λ_{abs}/nm	λ_{em}/nm
free radical and cation	350	533, 560 (τ = 285 ns, ϕ = 0.18)	500	515 (fluorescence) (τ < 4 ns, ϕ = 0.27) 600 (phosphorescence)
distonic 1,4-radical cation	350	530, 560 (τ = 189 ns, ϕ = 0.12)	500	535(fluorescence) (τ < 4 ns, ϕ = 0.12) 630 (phosphorescence)
distonic 1,6-peroxyl radical cation	nd	nd	350, 520	560 (fluorescence)

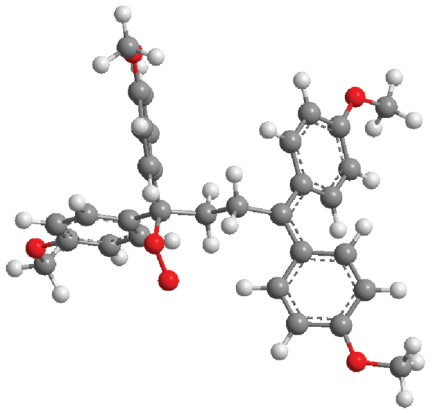

FIGURE 11. Optimized structure of 1,6-peroxyl radical cation of $DAE_2^{\bullet+}$ obtained by the density functional theory at the UB3LYP/6-31G* level.

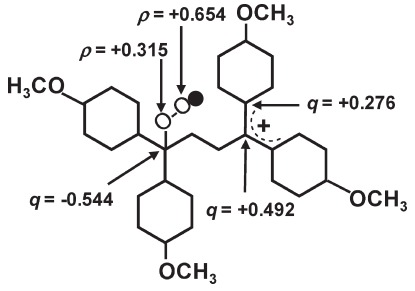

FIGURE 12. Select spin and charge densities (ρ and q, respectively) of 1,6-distonic peroxyl radical cation of $DAE_2^{\bullet+}$ obtained by the density functional theory at UB3LYP/6-31G* level.

of a 1,6-distonic peroxyl radical cation shifted to wavelengths longer than those of the 1,4-distonic radical cation. These behaviors perhaps suggest that slight through-space electronic interaction exists between an unpaired electron on oxygen and the cation site of the 1,6-distonic peroxyl radical cation in the ground and excited states. However, the spin and positive charge are separated on the peroxyl oxygen of subunit I and in subunit II, respectively.

Consequently, 1,4- and 1,6-acyclic distonic radical cations display characteristic distonic structures with separated radical and charge sites in the ground and excited states.

Conclusions

Absorption and emission measurements enabled us to confirm the properties of aromatic acyclic distonic radical cations in the ground and excited states, which are classified to bimodal reactive species in contrast to usual reactive species, such as free radical and cation. This is the first example to show the bimodal absorption and emissions of acyclic distonic radical cation in which spin and positive charge are separately localized. It is found that the electronic interaction between bond-deficient groups such as radical and cation linked by an ethylene chain is not strong in the ground and excited states. Therefore, our results provide meaningful information not only for a new perspective on radical cation but also for the molecular design of functionalized intermediates, such as a distonic radical cation with unique electronic structure.

Experimental Section

Materials. 1,1-Bis(4-methoxyphenyl)ethylene (DAE) was prepared by a Wittig reaction of $(p\text{-}CH_3OC_6H_4)_2CO$ with $(C_6H_5)_3P{=}CH_2$ and purified by column chromatography (silica gel) and recrystallization from *n*-hexane. HPLC grade BN was used as solvent without further purification. *n*-BuCl was shaken with concentrated sulfuric acid, washed with water, dried over calcium chloride, and fractionally distilled.

Pulse Radiolysis. Pulse radiolysis experiments were performed using an electron pulse (28 MeV, 8 ns, 0.87 kGy per pulse) from a linear accelerator at Osaka University. All experiments were performed in PhCN saturated with argon for 20 min. A 1-mL solution was placed in a quartz cell (10 mm × 5 mm × 40 mm) and sealed with a silicon rubber stopper. The kinetic measurements were performed using a nanosecond photoreaction analyzer system (Unisoku, TSP-1000). The monitor light was obtained from a pulsed 450-W Xe arc lamp (Ushio, UXL-451-0), which was operated by a large current pulsed power supply that was synchronized with the electron pulse. The monitor light was passed through an iris with a diameter of 0.2 cm and sent into the sample solution at a perpendicular intersection to the electron pulse. The monitor light passing through the sample was focused on the entrance slit of a monochromator (Unisoku, MD200) and detected with a photomultiplier tube (Hamamatsu Photonics, R2949). The transient absorption spectra were measured using a photodiode array (Hamamatsu Photonics, S3904-1024F) with a gated image intensifier (Hamamatsu Photonics, C2925-01) as a detector.

The kinetic traces in the near-infrared region were estimated using a fast InGaAs PIN photodiode with a monochromator (Horiba, TRIAX190) and the transient digitizer. The total system was controlled with a personal computer via GPIB interface.

γ-Radiolysis. The γ-radiolysis of the rigid glass of degassed *n*-butyl chloride solutions was carried out in 2 mm thick Suprasil cells in liquid nitrogen at 77 K by a ^{60}Co γ source (dose, 4.5×10^6 Gy). The absorption spectra were measured in a Dewar vessel at 77 K and also during the annealing up to approximately 100 K by a multichannel photodetector (Shimadzu, MultiSpec-1500).

The fluorescence and phosphorescence spectra were measured at 77 K by a fluorescence spectrophotometer (Hitachi, 850). The fluorescence lifetime was measured at 77 K by a single photon counting (Horiba, NAES-1100).

Theoretical Calculations. Optimized structure of 1,6-peroxy radical cation of DAE_2^+ was estimated by density functional theory at the UB3LYP/6-31G* level using the Gaussian03 package.

Acknowledgment. We thank the members of the Research Laboratory for Quantum Beam Science of ISIR, Osaka University for assistance in pulse radiolysis and γ-ray radiolysis experiments. This work has been partly supported by a Grant-in-Aid for Scientific Research (Projects 17105005, 21350075, 22245022, Priority Research (477) and others) from the Ministry of Education, Culture, Sports, Science and Technology (MEXT) of Japanese Government. S.T. thanks the Special Coordination Funds for Promoting Science and Technology from MEXT for the Osaka University Program for the Support of Networking among Present and Future Women Researchers. T.M. thanks the WCU (World Class University) program through the National Research Foundation of Korea funded by the Ministry of Education, Science and Technology (R31-10035) for support.

Supporting Information Available: Optimized molecular structure of 1,6-distonic peroxyl radical cation of $DAE_2^{\bullet+}$. This material is available free of charge via the Internet at http://pubs.acs.org.